INL/CON-15-36180
PREPRINT

An Analytical Methodology to Evaluate Thermal-hydraulic Performance of Compact Heat Exchangers, Accounting for Heat Loss

International Congress on Advances in Nuclear Power Plants (ICAPP 2016)

Su-Jong Yoon, James O'Brien, Piyush Sabharwall
(Idaho National Laboratory)

Kevin Wegman and Xiaodong Sun
(The Ohio State University)

April 2016

The INL is a
U.S. Department of Energy
National Laboratory
operated by
Battelle Energy Alliance

Proceedings of ICAPP 2016
April 17-20, 2016 – San Francisco, CA
Paper 15814

AN ANALYTICAL METHODOLOGY TO EVALUATE THERMAL-HYDRAULIC PERFORMANCE OF COMPACT HEAT EXCHANGERS, ACCOUNTING FOR HEAT LOSS

Su-Jong Yoon [a*], Kevin Wegman [b], James O'Brien [a], Piyush Sabharwall [a], and Xiaodong Sun [b]
[a] *Idaho National Laboratory, 2525 Fremont Ave., Idaho Falls, ID 83415*
Tel: 208-526-5407, Fax: 208-526-2930, Email: sujong.yoon@inl.gov
[b] *Nuclear Engr. Program, The Ohio State Univ., 201 W. 19th Ave., Columbus, OH 43210*

Abstract – *For the successful deployment of AHTR system, effective and robust high-temperature heat transport systems is essential. Printed circuit heat exchangers are strong candidate heat exchangers for intermediate loop or secondary loop of AHTR due to its high power density and compactness. Recently, Idaho National Laboratory has been developing the ARTIST facility to evaluate the thermal-hydraulic performance of PCHEs. The experimental data from that facility will be used as the basis for validation of CFD simulation for PCHE. In this work, the analytical methodology to evaluate the thermal-hydraulic performance of PCHE accounting for heat loss is developed because the extraneous heat losses from heat exchanger have an influence on the experimental data. In order to correctly compare experimental data with the simulation results, the heat loss from heat exchanger must be determined and incorporated. We employed the experimental data from straight-channel PCHEs with a high temperature and pressure helium gases using HTHF at the Ohio State University. The effectiveness of heat exchanger without accounting for heat loss was significantly dispersed whereas it showed a good agreement with the effectiveness evaluated by ε-NTU method when the developed methodology is employed. This methodology would be used for the improved evaluation of the heat exchanger performance, even though the heat loss of heat exchanger was not quantified experimentally.*

I. INTRODUCTION

Effective and robust high-temperature heat transport systems are fundamental to successful deployment of Advanced High Temperature Reactor (AHTR) systems for both power generation and nonelectric applications. Printed Circuit Heat Exchangers (PCHEs) are strong candidate heat exchangers for intermediate heat transport loops due to their very high power density, requiring much less material per unit of heat duty compared to conventional shell and tube heat exchangers. Idaho National Laboratory (INL) has been developing a computer code for the PCHE design and analysis [1], and will construct the Advanced Reactor Technology Integral System Test (ARTIST) facility to evaluate the thermal hydraulic performance of PCHEs [2]. The experimental data from the ARTIST facility will be used as the basis for validation of Computational Fluid Dynamics (CFD) simulations. In order to correctly compare experimental results with the simulations, the extraneous heat losses from the PCHEs must be determined and incorporated. These heat exchangers operate at high temperature and consequently, despite the use of external thermal insulation, experience non-negligible heat losses to the surroundings. The objective of this work is to develop an analytical methodology for quantification of these heat losses based on experimental data to evaluate and predict the performance of the heat exchanger accurately.

II. PCHES IN OSU HTHF

In an earlier study, performance data were acquired from straight-channel PCHEs with a high-temperature and high-pressure helium working fluid using the High-Temperature Helium test Facility (HTHF) at The Ohio State University (OSU) [3, 4]. Figure 1 shows the photo-chemically etched metal plates of the OSU PCHE. In this study, the experimental data from the straight-channel

PCHE of OSU has been used for reference data. Figure 2 shows instrumentation and component layout of the OSU HTHF. In this facility, two PCHEs, which have a same design, were installed to evaluate their performances for intermediate and high temperature conditions. There is an elbow upstream of the pressure gauge (10a in Fig.2) for PCHE1 hot side. The influence of this elbow on the experimental data will be discussed.

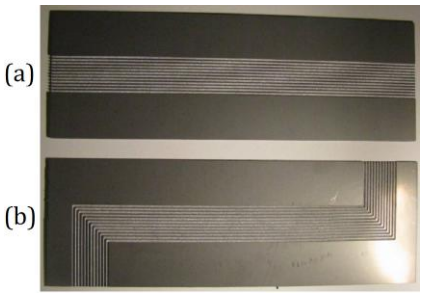

Fig. 1. Straight pattern and z-pattern of etched plates ((a) cold channel, (b) hot channel) [3]

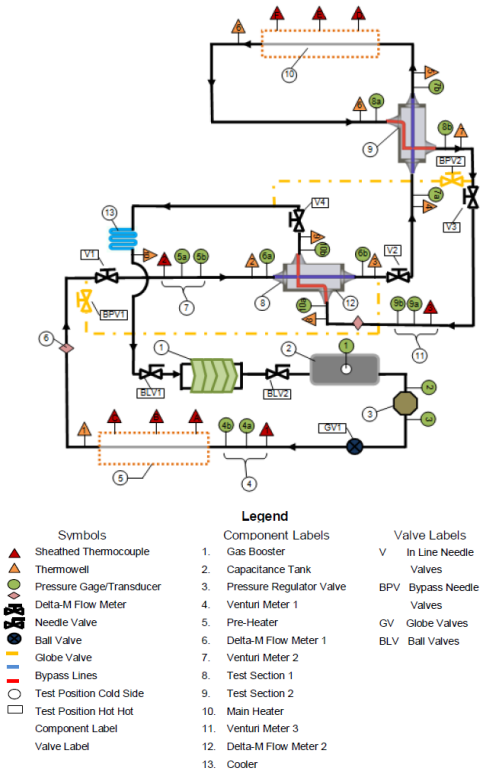

Fig. 2. Instrumentation and component layout for HTHF [4]

The OSU PCHEs were fabricated from 1.63 mm Alloy 617 plates with 2.0 mm diameter semi-circular flow channels etched into one surface of each plate with a channel pitch of 2.5 mm. Each plate had 10 hot and 10 cold plates with 12 channels per plate. The hot-side plate included two 90-degree bends plus a straight center section for a total flow length of 305 mm. The cold channels were straight-through with a flow length of 272 mm. The design parameters of the OSU PCHE are tabulated in Table I.

Table I: Design Parameters of OSU PCHE [3]

Parameter	Hot Side	Cold Side
Channel pitch (mm)	2.5	2.5
Channel width (mm)	2.0	2.0
Plate thickness (mm)	1.63	1.63
Hydraulic diameter (mm)	1.22	1.22
Channel travel length (mm)	305	272
Number of plates	10	10
Number of channels in each plate	12	12
Channel cross section area (mm^2)	1.57	1.57
Free flow area (mm^2)	188.4	188.4

III. HEAT EXCHANGER PERFORMANCE ANALYSIS

In the OSU experiments to evaluate PCHE performance, the measured variables, such as inlet and outlet temperatures, mass flow rates and pressures were employed with analytical method such as *ε-NTU* method [4]. However, these methods do not take account for heat loss from the heat exchangers, which can significant since these heat exchangers operate at high temperature. Hence the heat duty of heat exchanger based on the experimental data will be overestimated when these methods are employed without consideration of the heat loss. This section presents an analytical method to determine the heat duty of the heat exchanger accounting for the heat loss to the surroundings. For this analysis, it is assumed that only the inlet and outlet temperatures, mass flow rates and pressures of hot and cold fluids are known from the experiment. Figure 3 shows a heat balance between the hot and cold fluids, accounting for heat loss to the surroundings.

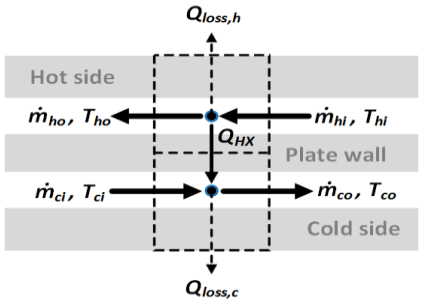

Fig. 3. Schematic diagram of heat balance of the heat exchanger considering heat losses

For the control volume around the hot-side fluid, using the sign convention for heat transfer indicated in the figure, energy conservation requires:

$$\begin{aligned}\dot{Q}_{net,h} &= Q_{loss,h} + Q_{HX} \\ &= \left(\dot{m}c_p\right)_h \left(T_{hi} - T_{ho}\right) = C_h \Delta T_h\end{aligned} \quad (1)$$

Similarly, for the cold side,

$$\begin{aligned}\dot{Q}_{net,c} &= Q_{HX} - Q_{loss,c} \\ &= \left(\dot{m}c_p\right)_c \left(T_{co} - T_{ci}\right) = C_c \Delta T_c\end{aligned} \quad (2)$$

where C_h and C_c are the heat capacity rates of hot and cold fluids, respectively.

Based on these energy balances, the heat loss from the heat exchanger can be determined in consideration of the combined hot and cold control volumes:

$$Q_{loss} = Q_{loss,h} + Q_{loss,c} = C_h \Delta T_h - C_c \Delta T_c \quad (3)$$

Consequently, the heat duty of heat exchanger, Q_{HX}, could be expressed by:

$$Q_{HX} = C_h \Delta T_h - Q_{loss,h} = C_c \Delta T_c + Q_{loss,c} \quad (4)$$

Here, a heat loss ratio, λ, is defined to determine the relative heat loss from each fluid.

$$Q_{loss,h} = \lambda Q_{loss} \quad (5)$$

$$Q_{loss,c} = \left(1-\lambda\right) Q_{loss} \quad (6)$$

where $0 \le \lambda \le 1$.

Assuming heat conduction and natural convection are the primary mechanisms of extraneous heat loss, the heat loss for each channel should be proportional to the temperature difference between the fluid and the ambient laboratory atmosphere. Hence, the heat loss ratio can be estimated from the averaged temperatures of each fluid and the ambient temperature as following:

$$\frac{Q_{loss,h}}{Q_{loss,c}} = \frac{\lambda Q_{loss}}{\left(1-\lambda\right) Q_{loss}} = \frac{T_{h,avg} - T_\infty}{T_{c,avg} - T_\infty} \quad (7)$$

which yields

$$\lambda = \frac{T_{h,avg} - T_\infty}{T_{h,avg} + T_{c,avg} - 2T_\infty} \quad (8)$$

where the averaged temperatures of the hot and cold fluids are determined by:

$$T_{h,avg} = \frac{1}{2}\left(T_{ho} + T_{hi}\right) \quad (9)$$

$$T_{c,avg} = \frac{1}{2}\left(T_{co} + T_{ci}\right) \quad (10)$$

The heat duty of the heat exchanger can be also expressed in terms of the overall heat transfer coefficient (U), overall heat transfer surface area (A) and Log Mean Temperature Difference (LMTD, ΔT_{LM}):

$$Q_{HX} = UA\Delta T_{LM} \quad (11)$$

For a counterflow heat exchanger, the LMTD is defined by:

$$\Delta T_{LM} = \frac{\left(T_{hi} - T_{co}\right) - \left(T_{ho} - T_{ci}\right)}{\ln\left(\dfrac{T_{hi} - T_{co}}{T_{ho} - T_{ci}}\right)} \quad (12)$$

From Eqs. (3)-(6), the heat duty of heat exchanger could be expressed by:

$$Q_{HX} = \left(1-\lambda\right) C_h \Delta T_h + \lambda C_c \Delta T_c \quad (13)$$

From Eq. (11) and Eq.(13), the product of overall heat transfer coefficient and overall heat transfer surface area is determined by:

$$UA = \frac{\left(1-\lambda\right) C_h \Delta T_h + \lambda C_c \Delta T_c}{\Delta T_{LM}} \quad (14)$$

The Number of Transfer Unit (NTU) is determined as follows:

$$NTU \equiv \frac{UA}{C_{\min}} = \frac{\left(1-\lambda\right) C_h \Delta T_h + \lambda C_c \Delta T_c}{C_{\min} \Delta T_{LM}} \quad (15)$$

where the minimum heat capacity rate of heat exchanger C_{min} is determined by:

$$C_{\min} = \min\left(C_h, C_c\right) \quad (16)$$

Consequently, the empirical effectiveness of the heat exchanger is determined as follows:

$$\varepsilon \equiv \frac{Q_{HX}}{Q_{\max}} = \frac{(1-\lambda)C_h\Delta T_h + \lambda C_c \Delta T_c}{C_{\min}(T_{hi} - T_{ci})} \quad (17)$$

IV. THE COLBURN ANALOGY

Colburn *j*-factor is used to characterize transport phenomena occurring in the heat exchanger. The Colburn *j*-factor is defined by:

$$j \equiv St \cdot Pr^{2/3} = \frac{Nu}{Re \cdot Pr^{1/3}} \quad (18)$$

where *Nu* is Nusselt number, *Pr* is Prandtl number and *St* is Stanton number.

The definitions of the dimensionless variables in Eq.(18) are given by:

Stanton number: $$St \equiv \frac{h}{\rho c_p u} = \frac{hA_{x-s}}{\dot{m} c_p} \quad (19)$$

Nusselt number: $$Nu \equiv \frac{hD_{hy}}{k} \quad (20)$$

Prandtl number: $$Pr \equiv \frac{\nu}{\alpha} = \frac{c_p \mu}{k} \quad (21)$$

where D_{hy} is the hydraulic diameter of semi-circular channel of PCHE and A_{x-s} is the cross-sectional area of the flow channel.

To determine the Colburn *j-factor* for the given heat exchanger, the convective heat transfer coefficient (*h*) must be determined first. In this study, the mean convective heat transfer coefficient of the heat exchanger is used to determine the Colburn *j-factor*. The mean convective heat transfer coefficient for each channel is determined by:

$$\bar{h}_h = \frac{-Q_{HX}}{A_h \Delta T_{LM,h}} \quad (22)$$

$$\bar{h}_c = \frac{Q_{HX}}{A_c \Delta T_{LM,c}} \quad (23)$$

where A_h and A_c are the heat transfer surface areas, $\Delta T_{LM,h}$ and $\Delta T_{LM,c}$, the local LMTDs of the hot and cold channels.

The local LMTD of each channel is determined by:

$$\Delta T_{LM,h} = \left(\frac{\Delta T_o - \Delta T_i}{\ln(\Delta T_o / \Delta T_i)} \right)_h \quad (24)$$

$$\Delta T_{LM,c} = \left(\frac{\Delta T_o - \Delta T_i}{\ln(\Delta T_o / \Delta T_i)} \right)_c \quad (25)$$

and

$$\Delta T_o = (T_w - T_m)_o \quad (26)$$

$$\Delta T_i = (T_w - T_m)_i \quad (27)$$

where T_w is the wall temperature and T_m is the mean (bulk) temperature of fluid.

If the temperature difference across the wall separating the hot and cold channels is negligible, it can be assumed that the temperature across the wall is constant. Since the wall thickness between the hot and cold channels in PCHE is very small, and the heat transfer mechanism in the wall is conduction, the wall temperature at any axial location can be estimated by averaging the bulk temperatures of hot and cold fluids at that location. Therefore, the wall temperature is determined by:

$$T_w(x) = \frac{T_{m,h}(x) + T_{m,c}(x)}{2} \quad (28)$$

For the counterflow heat exchanger, the mean temperature of the wall at each end could be expressed as follows:

$$(T_{wo})_h = (T_{wi})_c = \frac{T_{ho} + T_{ci}}{2} \quad (29)$$

$$(T_{wi})_h = (T_{wo})_c = \frac{T_{hi} + T_{co}}{2} \quad (30)$$

Substituting Eq.(29) and Eq.(30) into Eq.(26) and Eq.(27) yields the temperature differences between the fluid and wall at the inlet and outlet as follows:

$$(\Delta T_o)_h = (T_{wo})_h - T_{ho} = \frac{T_{ci} - T_{ho}}{2} \quad (31)$$

$$(\Delta T_i)_h = (T_{wi})_h - T_{hi} = \frac{T_{co} - T_{hi}}{2} \quad (32)$$

$$(\Delta T_o)_c = (T_{wo})_c - T_{co} = \frac{T_{hi} - T_{co}}{2} \quad (33)$$

$$(\Delta T_i)_c = (T_{wi})_c - T_{ci} = \frac{T_{ho} - T_{ci}}{2} \quad (34)$$

Substituting Eqs.(31)-(34) into Eqs.(24) and (25) yields the local LMTD of each channel:

$$\Delta T_{LM,h} = \left(\frac{\Delta T_o - \Delta T_i}{\ln\left(\Delta T_o / \Delta T_i\right)} \right)_h = \frac{\Delta T_h - \Delta T_c}{2\ln\left(\frac{T_{ci} - T_{ho}}{T_{co} - T_{hi}} \right)} \quad (35)$$

$$\Delta T_{LM,c} = \left(\frac{\Delta T_o - \Delta T_i}{\ln\left(\Delta T_o / \Delta T_i\right)} \right)_c = \frac{\Delta T_h - \Delta T_c}{2\ln\left(\frac{T_{hi} - T_{co}}{T_{ho} - T_{ci}} \right)} \quad (36)$$

Consequently, the mean convective heat transfer coefficient of each channel could be determined by:

$$\bar{h}_h = \frac{(\lambda - 1)C_h \Delta T_h - \lambda C_c \Delta T_c}{\left(A_h / 2\right)\left(\Delta T_h - \Delta T_c\right)} \ln\left(\frac{T_{ci} - T_{ho}}{T_{co} - T_{hi}} \right) \quad (37)$$

$$\bar{h}_c = \frac{(1 - \lambda)C_h \Delta T_h + \lambda C_c \Delta T_c}{\left(A_c / 2\right)\left(\Delta T_h - \Delta T_c\right)} \ln\left(\frac{T_{hi} - T_{co}}{T_{ho} - T_{ci}} \right) \quad (38)$$

Apart from the heat transfer characteristics, the pressure loss also has to be looked at and is an important factor to determine required pumping power. For the Colburn analogy to determine the transport characteristics of heat exchanger, the frictional loss needs to be analyzed. However, it is very difficult to measure the frictional loss directly. The only pressure data that could be measured in the experiment was the overall pressure drop across the heat exchanger. The overall pressure drop of the PCHE measured in the experiment includes the frictional loss, form losses at the inlet and outlet plenums (entrance and exit losses), form loss due to the bends in the channel and a minor loss due to the flow acceleration (or deceleration). Hence the measured overall pressure drop is given by:

$$\Delta P_{net} = \Delta P_{fric} + \sum \Delta P_{form} + \Delta P_{accel} \quad (39)$$

Since the hot channel has two 90-degree bends, the total pressure loss of hot fluid side is bigger than the cold fluid side that is a straight channel. The respective form losses of the hot and cold channels are given by:

$$\Delta P_{form,h} = \Delta P_{Ent} + \Delta P_{Bends} + \Delta P_{Ext} \quad (40)$$

$$\Delta P_{form,c} = \Delta P_{Ent} + \Delta P_{Ext} \quad (41)$$

The form loss at the entrance consists of the pressure loss due to the area change at the entrance and irreversible momentum loss associated with the flow separation and secondary flow at the vena contracta. Hence the form loss at the entrance is given by:

$$\Delta P_{Ent} = \left(1 - \sigma^2 + K_c\right)\left(\frac{G^2}{2\rho_i} \right) \quad (42)$$

where ρ_i is fluid density at the entrance, G is the mass flux of fluid flow, σ is the ratio of core free-flow area to frontal area, and K_c is contraction loss coefficient. For the OSU PCHE design, σ is 0.087 and K_c is 0.5 [5].

In the similar manner, the form loss at the exit is given by:

$$\Delta P_{Ext} = \left(1 - \sigma^2 - K_e\right)\left(\frac{G^2}{2\rho_o} \right) \quad (43)$$

where ρ_o is fluid density at the exit, and K_e is exit loss coefficient (=0.85) [5].

The form loss due to the bends in the hot channel can be estimated by:

$$\Delta P_{Bend} = K_{Bend} \frac{\left(\rho_i + \rho_o\right)}{\rho_o}\left(\frac{G^2}{2\rho_i} \right) \quad (44)$$

where K_{Bend} is the form loss coefficient due to the bend (=1.202) [6].

The minor loss due to the flow acceleration or deceleration is given by:

$$\Delta P_{accel} = \left(\frac{G^2}{2\rho_i} \right) 2\left(\frac{\rho_i}{\rho_o} - 1 \right) \quad (45)$$

The frictional losses of hot and cold side are given by:

$$\Delta P_{fric,h} = \left(\frac{G^2}{2\rho_i} \right)_h 4 f_h \frac{L_h}{D_{hy}} \left(\frac{\left(\rho_i + \rho_o\right)}{2\rho_o} \right)_h \quad (46)$$

$$\Delta P_{fric,c} = \left(\frac{G^2}{2\rho_i} \right)_c 4 f_c \frac{L_c}{D_{hy}} \left(\frac{\left(\rho_i + \rho_o\right)}{2\rho_o} \right)_c \quad (47)$$

From Eqs. (39)-(47), the friction factor of each side is determined by:

$$f_h = \frac{D_{hy}}{L_h} \left(\begin{array}{l} \left(\frac{\rho_i \Delta P_{net}}{\left(\rho^* + 1\right) G^2} \right) - \frac{\left(1 - \sigma^2\right)}{2} \\ + \frac{\left(\rho^* K_e - K_c\right)}{2\left(\rho^* + 1\right)} - \frac{K_{Bend}}{2} - \frac{\left(\rho^* - 1\right)}{\left(\rho^* + 1\right)} \end{array} \right)_h \quad (48)$$

$$f_c = \frac{D_{hy}}{L_c}\left(\left(\frac{\rho_i \Delta P_{net}}{\left(\rho^* + 1\right)G^2}\right) - \frac{\left(1-\sigma^2\right)}{2} + \frac{\left(\rho^* K_e - K_c\right)}{2\left(\rho^* + 1\right)} - \frac{\left(\rho^* - 1\right)}{\left(\rho^* + 1\right)}\right)_c \quad (49)$$

where ρ^* is the ratio of fluid densities at the inlet to the outlet ($\rho^*=\rho_i/\rho_o$), L_h and L_c are the travel lengths of hot and cold channels.

V. ANALYSIS OF OSU PCHE EXPERIMENTAL DATA

The experimental test matrix for the OSU PCHE experiments is tabulated in Table II. For the given experimental matrix, 141 tests were conducted.

Table II: OSU PCHE Experimental Matrix [3]

Parameter		PCHE1	PCHE 2
Pressure (MPa)	Cold	1.03-2.71	1.02-2.68
	Hot	0.98-2.6	1.01-2.66
Inlet temperature (^{o}C)	Cold	85-188	170-390
	Hot	208-376	297-790
Flow rate (kg/h)	Cold	15-49	15-49
	Hot	15-49	15-49
Reynolds number of channel	Cold	950-3750	800-3200
	Hot	950-3750	800-3200

The PCHE inlet temperature and pressure were varied from 85 to 390˚C and 1.03 to 2.71 MPa, respectively for the cold side and 208 to 790˚C and 1.02 to 2.68 MPa, respectively for the hot side, while the mass flow rate of helium was varied from 15 to 49 kg/h. This range of mass flow rates corresponds to PCHE channel Reynolds numbers of 950 to 3750 for the cold side and 800 to 3200 for the hot side (corresponding to the laminar and laminar-to-turbulent transition flow regimes).

The two PCHEs and the hot and cold sides of each PCHE were arranged in series such that the mass flow rates for each test were exactly the same for both PCHEs' and also for both sides. Since the specific heat of helium is constant, the heat capacity rates of hot and cold-side fluids were always the same for each test. Therefore, the minimum, hot and cold side heat capacity rates in Eq.(17) are same in this analysis.

Figure 4 shows the estimated heat losses for the hot and cold sides. The heat loss of the hot side is larger than that of cold side as expected. As the LMTD increases, not only the amount of heat loss increases, but also its distribution was spread out. Dispersed heat loss implies that the effectiveness of heat exchanger based on the experiment data without accounting heat loss would have large uncertainty.

The amount of heat loss cannot be neglected as shown in Fig. 5. The ratio of heat loss to the heat duty averaged ~5%, with some values as high as 21.5%. The performance of the heat exchanger cannot be evaluated correctly without considering the heat loss. Another reason why the heat loss should be considered is because unreasonable experimental data (unphysical data, as can be seen in Fig.4, bottom most data points) could be detected from the heat loss analysis. The amount of heat loss must be a positive value, because there is no mechanism for external heat addition to the heat exchanger. However, two cases which have apparent negative heat loss were observed in Figs. 4 and 5. Measurement errors in those cases must be investigated to ensure the validity of the experiment.

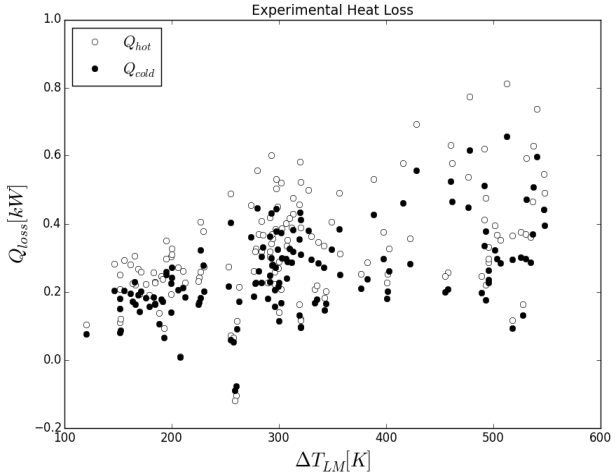

Fig. 4. Absolute heat loss in the OSU PCHE experiment

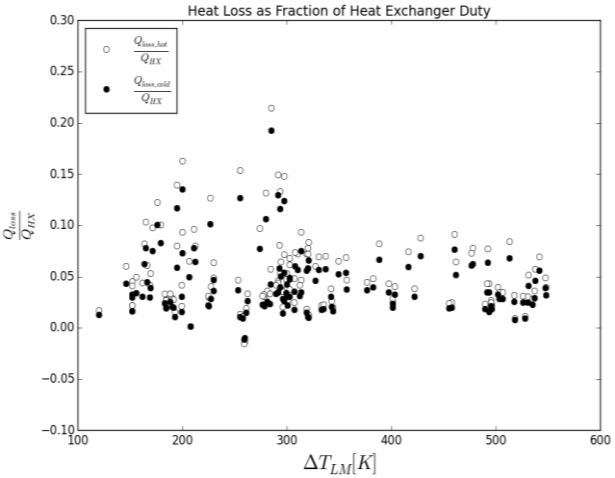

Fig. 5. Ratio of heat loss to heat duty in the OSU PCHE experiment

Generally, the *ε-NTU* method is used to determine the effectiveness of heat exchanger for given specifications and required operating conditions. As for

the counterflow heat exchanger, the effectiveness of heat exchanger is calculated by:

$$\varepsilon = \frac{1-\exp\left(-NTU\left(1-C_r\right)\right)}{1-C_r\exp\left(-NTU\left(1-C_r\right)\right)} \quad (50)$$

where C_r is the heat capacity ratio ($C_r = C_{min}/C_{max}$)

Figure 6 shows the effectiveness-NTU plot of the experimental data. The line in the figure is the analytical solution by *ε-NTU* method. As aforementioned, because the heat capacity rates of hot and cold sides in the OSU PCHE experiment were same, the heat capacity ratio of the experimental data is 1.0. The effectivenesses calculated based on the inlet and outlet temperatures without accounting heat loss were widely spread out whereas the effectiveness evaluated by Eq.(17) shows good agreement with the analytical solution. The experimental uncertainty associated with heat loss could be significantly reduced by this methodology. When the heat loss was not accounted, the effectiveness of hot side was overestimated while that of cold side was underestimated. These results are corresponding to the Nusselt number of each side.

The effectiveness evaluated by this methodology includes the effect of thermal insulation. The effectiveness of the OSU PCHE evaluated by this methodology ranged from 0.65 to 0.75. Generally, the effectiveness of heat exchanger for the industrial application is required to be higher than 0.85. In this aspect, the PCHE design needs to be improved to achieve its acceptable performance for the high temperature helium application.

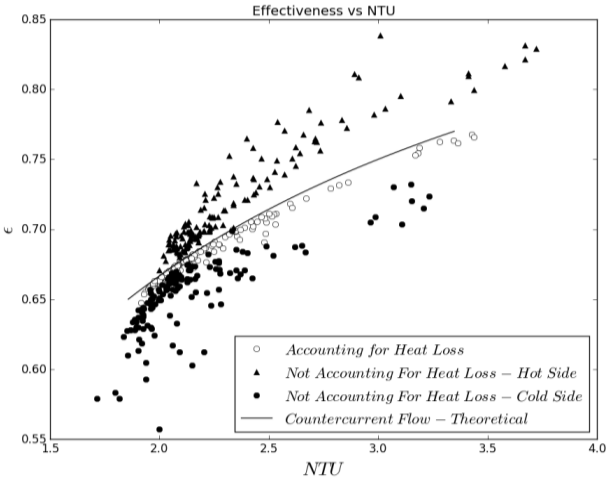

Fig. 6. Effectiveness-NTU plot of the OSU PCHE experiment

Figures 7 and 8 show the Nusselt numbers of hot and cold channels, respectively. The Nusselt number for the fully-developed laminar flow in a straight semi-circular channel is tabulated in Table III. T thermal boundary represents the constant wall temperature boundary everywhere, H1 thermal boundary represents uniform wall heat flux boundary axially with constant temperature circumferentially and H2 thermal boundary condition represents uniform wall heat flux but in the absence of peripheral wall conduction.

Table III: Nusselt Numbers in a Straight Semi-Circular Channel [7, 8, 9]

Boundary type	*Nu*
T thermal boundary [7]	3.323
H1 thermal boundary [8]	4.089
H2 thermal boundary [9]	2.923

The Nusselt number of the cold side in the laminar flow regime was slightly higher than that of H1 thermal boundary while that of hot side was between H1 and T thermal boundaries. Hesselgreaves [8] recommends using the Gnielinski correlation [10] for the semi-circular channel, which is valid for Reynolds number from 2300 to 5×10^6 and Prandtl number from 0.5 to 2000. The Gnielinski correlation for the semi-circular channel is given by:

$$Nu = \frac{\left(f/2\right)\left(Re-1000\right)Pr}{1+12.7\sqrt{f/2}\left(Pr^{2/3}-1\right)} \quad (51)$$

$$f = \frac{1}{4}\left(\frac{1}{1.8\log Re - 1.5}\right)^2 \quad (52)$$

As shown in Figs. 7 and 8, the experimental data shows a good agreement with Gnielinski correlation in the turbulent flow regime. We note that the Gnielinski correlation could predict the Nusselt number for Reynolds numbers lower than its stated limit. For the straight semi-circular channel, the Gnielinski correlation is deemed to be valid for Reynolds number from 1800.

The heat transfer characteristics of heat exchanger can be plotted in terms of Colburn *j*-factor as shown in Figs. 9 and 10. In the laminar regime, the Colburn j-factor agreed with that calculated with the Nusselt number of H1 boundary. In the transition regime from laminar to turbulent, the Colburn *j*-factor increases with increasing Reynolds number. Due to this effect of transitional flow, the Colburn *j*-factors for Reynolds numbers ranging from 1500 to 2000 were higher than the values calculated based on the Nusselt numbers for fully-developed laminar flow. As aforementioned, in the turbulent regime for Reynolds numbers over 1800, the Colburn *j*-factor in the turbulent regime shows a good agreement with the Gnielinski correlation.

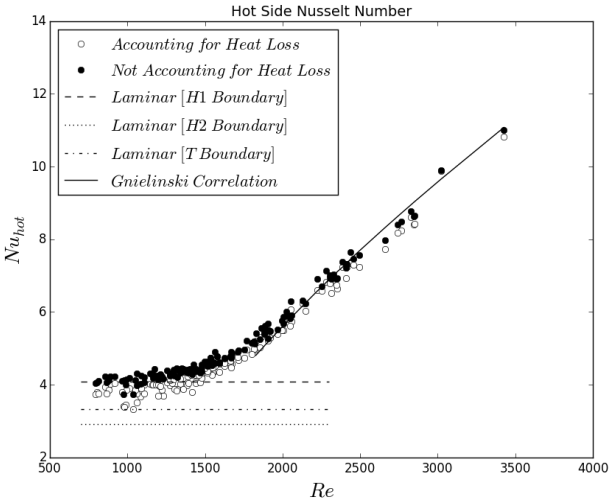

Fig. 7. Nusselt numbers on hot side of the OSU PCHE experiment

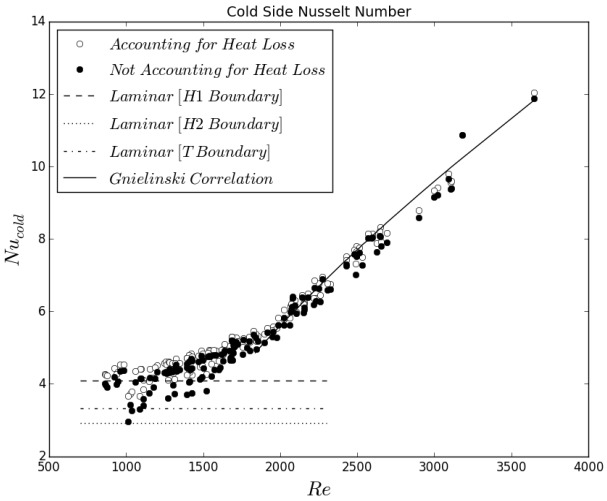

Fig. 8. Nusselt numbers on cold side of the OSU PCHE experiment

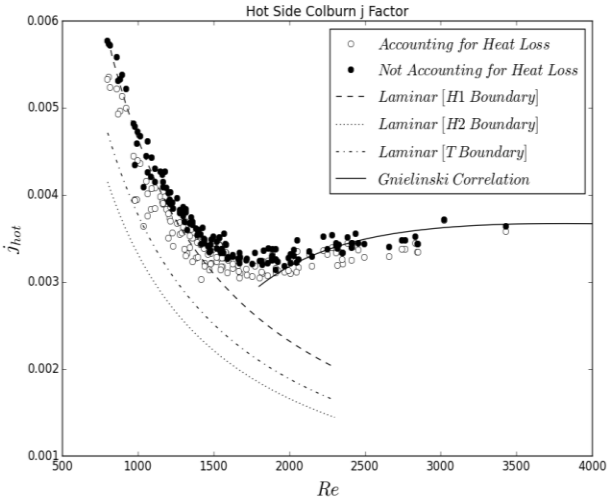

Fig. 9. Colburn *j*-factor on hot side

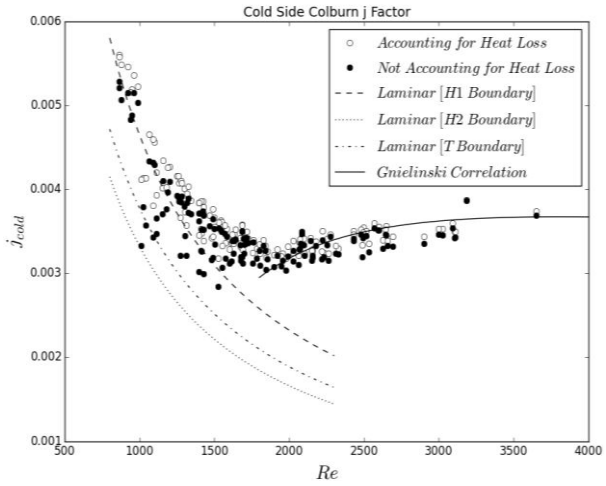

Fig. 10. Colburn *j*-factor on cold side

Figure 11 shows the friction factors as a function of Reynolds number on the hot and cold sides. The pressure loss on hot side shows two different trends. This is due to the configuration of the experimental facility. As shown in Fig.2, there is an elbow upstream of the pressure gauge for PCHE1 hot side. Mylavarapu [3] mentioned that this elbow causes an additional pressure drop on the hot side due to the effect of secondary flow. In this case, the location of the pressure sensor has a significant influence on the data. The pressure at this region is similar to the pressure change across an orifice. The local flow velocity affects the measured pressure. For instance, if the pressure tap is located inside of the elbow where the flow velocity is low, the measured pressure is higher than average value such that the pressure drop will be overestimated. Existing empirical correlations for the pressure drop across the bend are not available for estimating this local variation of flow velocity. Therefore, in a design point of view, the bend at the upstream of heat exchanger entrance should be avoided.

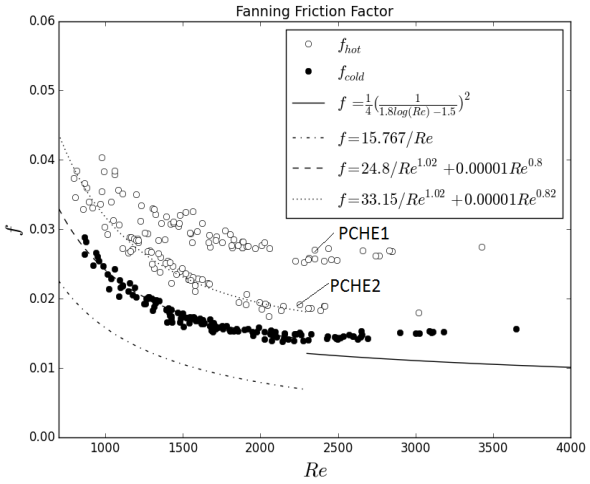

Fig. 11. Fanning friction factor of OSU PCHE experiment

As shown in figure above, turbulent friction factor correlations underestimated the friction factor in both transition and turbulent regimes. Since the OSU PCHE experimental conditions were concentrated in the laminar regime, additional experiments are required to investigate the performance of these PCHEs in the turbulent regime. In the laminar flow regime, Hesselgreaves [8] suggested that the product of friction factor and Reynolds number for fully developed laminar flow in a semicircular channel is 15.767. Because the size of flow channel is in the order of millimeter, fabricating tolerance has significant influence on the pressure loss of PCHE. However, it is practically impossible to inspect the inside of heat exchanger to figure out the reason why experimental friction factor is higher than that suggested by Hesselgreaves because PCHE is fabricated by the diffusion-bonding technique. As shown in Fig.11, theoretical friction factor correlation did not predict experimental data correctly. Hence, we fitted the curves which can predict the experimental fanning friction factor within the error of ± 7.0% as shown in Figs. 12 and 13. The empirical correlations for the friction factor of hot and cold side, valid for 860 ≤ Re ≤ 2300, are given by:

$$f_{correlation,cold} = \frac{24.8}{Re^{1.02}} + 0.00001Re^{0.8} \quad (53)$$

$$f_{correlation,hot} = \frac{33.15}{Re^{1.02}} + 0.00001Re^{0.82} \quad (54)$$

The correlation's shown in equations above are specific to the current geometry (as can be seen in Fig. 1) and further validation for other PCHE types needs to be carried out before a validated conclusion could be derived.

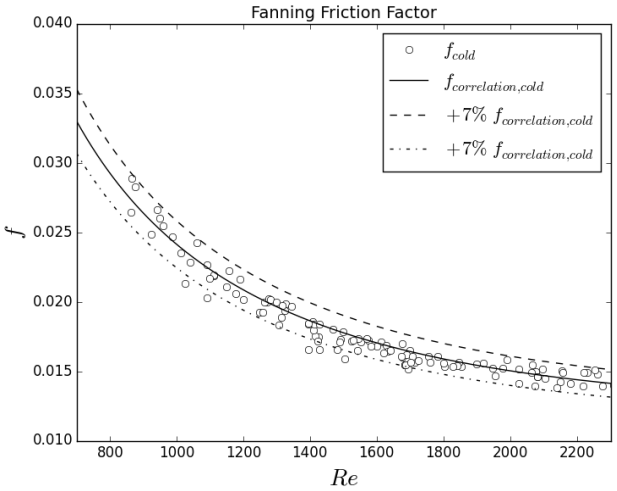

Fig. 12. Laminar friction factor correlation for cold side

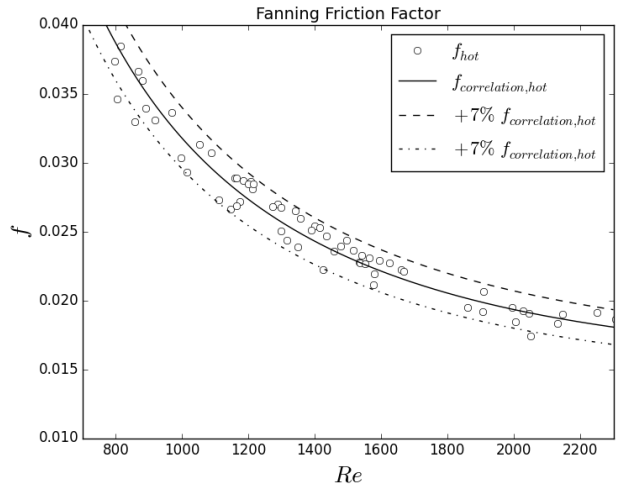

Fig. 13. Laminar friction factor correlation for hot side

VI. CONCLUSIONS

In this work, an analytical methodology was developed to evaluate the thermal-hydraulic performance of compact heat exchangers, specifically focusing on PCHEs, accounting for the heat loss from the heat exchanger. The experimental data of OSU PCHEs were analyzed by this methodology. The following points summarize the results:

- In order to evaluate the effectiveness of heat exchanger correctly, the heat loss of heat exchanger must be properly accounted. The experimental uncertainty was significantly reduced by accounting heat loss.
- Heat loss analysis provided the additional information establishing for the validity of the experiment. Unreasonable and unphysical experimental data could be detected by this methodology.
- Convective heat transfer coefficients of channel were derived by accounting heat loss to improve the accuracy of Colburn *j*-factor which is a major factor for determination of the thermal-hydraulic performance of heat exchanger.
- The empirical correlations for the laminar frictional loss showed a good accuracy within the error of ± 7%.

In conclusion, the developed methodology could be applied to evaluate the heat exchanger performance accurately, even though the heat loss of heat exchanger was not quantified experimentally.

NOMENCLATURE

A	Overall heat transfer surface area, m^2
C	Heat capacity rate ($=\dot{m}\cdot c_p$), W/K
c_p	Specific heat, J/(kg·K)
D	Diameter, m
f	Friction factor
G	Mass flux, kg/(m^2·sec)
h	Convective heat transfer coefficient, W/(m^2·K)
j	Colburn factor
k	Thermal conductivity, W/(m·K)
K_{Bend}	Form loss coefficient at bend
K_c	Contraction loss coefficient
K_e	Exit loss coefficient
L	Travel length, m
$\dot{m}$	Mass flow rate, kg/sec
NTU	Number of transfer unit
Nu	Nusselt Number
P	Pressure, Pa
Pr	Prandtl number
Q	Heat load, W
Re	Reynolds number
St	Stanton number
T	Temperature, K
U	Overall heat transfer coefficient, W/(m^2·K)
u	Flow velocity, m/sec
V	Volume, m^3
α	Thermal diffusivity, m^2/sec
Δ	Differential
ε	Effectiveness
λ	Heat loss ratio
μ	Dynamic viscosity, Pa·sec
ν	Kinematic viscosity, m^2/sec
ρ	Density, kg/m^3
ρ^*	Ratio of fluid densities at inlet to outlet
σ	Ratio of core free-flow area to frontal area

Subscript

accel	Acceleration
avg	Averaged
Bends	Bends
c	Cold fluid
Ent	Entrance
Ext	Exit
form	Form loss
fric	Frictional loss
h	Hot fluid
HX	Heat exchanger
hy	Hydraulic diameter
i	Inlet
LM	Log mean temperature difference
loss	Heat loss
m	Bulk
max	Maximum
min	Minimum
net	Total
o	Outlet
w	Wall
x-s	Cross-sectional
∞	Ambient

REFERENCES

1. S. J. Yoon, P. Sabharwall, and E. S. Kim, Analytical Study on Thermal and Mechanical Design of Printed Circuit Heat Exchanger, INL/EXT-13-30047, Idaho National Laboratory, Idaho Falls, ID, 2013.
2. J. E. O'Brien, P. Sabharwall, and S. J. Yoon, A Multi-Purpose Thermal Hydraulic Test Facility for Support of Advanced Reactor Technologies, 2014 ANS Winter Meeting, Nov. 9-13, 2014, Anaheim, CA.
3. S. K. Mylavarapu, Design, Fabrication, Performance Testing, and Modeling of Diffusion Bonded Compact Heat Exchanger in a High-Temperature Helium Test Facility, Ph.D Thesis, Ohio State University, 2011.
4. R. E. Glosup, Characterization of the High-Temperature Helium Facility in the Thermal Hydraulics Laboratory, B.S. Thesis, Ohio State University, 2011.
5. R. K. Shah, D. P. Sekulic, Fundamentals of Heat Exchanger Design, John Wiley & Sons, Inc., Hoboken, New Jersey, 2003.
6. D. C. Rennels, and H. M. Hudson, Pipe Flow: A Practical and Comprehensive Guide, p.168, Wiley, Hoboken, NJ, 2012.
7. N. R. Rosaguti, D. F. Fletcher, and B. S. Haynes, Laminar flow and heat transfer in a periodic serpentine channel with semi-circular cross-section, International Journal of Heat and Mass Transfer, Vol.49 (17–18), pp.2912–2923, 2006.
8. J. E. Hesselgreaves, Compact Heat Exchanger, Pergamon, London, UK, 2001.
9. R. K. Shah and A. L. London, Advances in Heat Transfer, Academic Press, New York, 1978.
10. F. P. Incropera, D. P. DeWitt, Fundamentals of Heat and Mass Transfer (6th ed.), Wiley, Hoboken, NJ, 2007.